Journal of Solid Mechanics Vol. 14, No. 3 (2022) pp. 345-360
DOI: 10.22034/jsm.2021.1928249.1690

Research Paper

A Novel Spring-Based Model for Damage Investigation of Functionally Graded Beams

S. Karimi [1], M. Bozorgnasab [1,*], R. Taghipour [1], M.M. Alipour [2]

[1]*Department of Civil Engineering, Faculty of Engineering and Technology, University of Mazandaran, Babolsar, Iran*
[2]*Department of Mechanical Engineering, Faculty of Engineering and Technology, University of Mazandaran, Babolsar, Iran*

Received 29 May 2022; accepted 5 July 2022

ABSTRACT

In this paper, free vibration analysis of damaged functionally graded beams based on the first-order shear deformation theory (FSDT) is carried out. In this regard, a new model of springs is introduced to model the damaged elements of the beam. The proposed model is achieved from stress resultants. The springs equations for homogeneous and functionally graded (FG) beams are presented; furthermore, equations for equivalent springs are also provided which can be used for both homogeneous and FG beams. The proposed method can be applied for the analysis of structures with fewer computation costs and high accuracy. To show the accuracy of the proposed model, the natural frequencies of the beams with real elements and the ones which are modeled by the proposed springs are compared considering various support conditions. Good agreement has been observed. Thereafter, the model is used to detect the damaged elements. The result shows that the model can properly detect the damage location.

Keywords : Functionally graded beam; Free vibration analysis; Damage detection; First-order shear deformation theory; Spring.

1 INTRODUCTION

STRUCTURAL health monitoring is essential for the identification of damages and integrity of structures. Health monitoring can be categorized in four main steps: determination of damage existence, defining its location, identification of the damage severity, and finally, the prediction of the remaining lifetime of the damaged structure [1]. The beam is one of the basic members of a structure; therefore, identification of the damage in the beam, especially the functionally graded beam, which is a new type of composite beams, is of great importance. One of the most common methods in damage detection is the use of modal data and free vibration analysis, which have been widely studied in recent years [2,3,4]. In 1995, Wu and Huang studied free vibration and forced dynamic responses of a beam based on the analytical and numerical combined methods. The beam was a uniform cantilever

*Corresponding author. Tel.: +98 1135302903.
E-mail address: m.bozorgnasab@umz.ac.ir (M. Bozorgnasab)

Timoshenko beam and subjected to several loads with various masses and translational and rotational springs [2]. In 1998, based on continuous cracked beam vibration theory and fracture mechanics methods, Chondros et al. studied lateral vibration of Euler-Bernoulli beams with open cracks and also a steel beam with a double-edge crack [3]. Li investigated free vibration analysis of a beam by a simple and unified approach and showed the efficiency of the proposed technique by numerical examples [4]. In 2003, Patil and Maiti investigated the crack detection in Euler-Bernoulli beams by modeling the crack with a rotational spring based on frequency measurements. The efficiency of their proposed method was shown through numerical studies and evaluation of the differences between the locations and sizes of the predicted crack and the actual one [5]. Lu and Chen investigated free vibration of functionally graded beams based on the two-dimensional theory of elasticity and a hybrid state-space/differential quadrature method. They verified their method by comparison with an exact solution of the FG beam [6]. In 2007, Aydogdu and Taskin surveyed the free vibration analysis of a FG beam with simply supported edges based on different higher-order shear deformation and classical beam theories [7]. Sina et al. studied free vibration analysis of functionally graded beams based on an analytical method. They investigated the effects of different conditions on natural frequencies and mode shapes of the FG beams [8]. In 2010, Simsek investigated vibration analysis of the FG beam based on Euler–Bernoulli, Timoshenko, and the third-order shear deformation beam theories. The beam was simply-supported and under a moving mass. He studied the effects of various conditions, such as various material distributions on the dynamic response of the beam [9]. Moradi et al. studied the crack identification in beams based on the bees algorithm. A rotational spring was used to model the crack. The size and location of the crack were well predicted by this method [10]. More recently, Manoach et al. presented a numerical and experimental study of the vibration-based damage detection in laminated beams under temperature variations and dynamic loads using Poincare maps. Experimental tests confirmed the efficiency of the proposed method [11]. In 2013, Pradhan and Chakraverty investigated free vibration of the functionally graded beams with different boundary conditions based on the classical and first-order shear deformation beam theories. They studied the effects of various boundary conditions and different beam theories on the natural frequencies of the beams [12]. Wattanasakulpong and Ungbhakorn studied linear and nonlinear vibration analysis of functionally graded porous beams with elastically restrained edge based on the differential transformation method (DTM). They presented linear and nonlinear frequencies of the beam based on different material property distributions, porosity, and spring constants [13]. By using DTM and based on the first order shear deformation theory, Shariyat and Alipour [14,15] and Alipour and Shariyat [16,17] analyzed undamaged non-homogeneous circular plates. In 2015, Yazdanpanah and and seyedpoor introduced a damage indicator for beams based on mode shape, mode shape slope, and mode shape curvature. The proposed indicator determined the location of damage, properly [18]. In another paper, Chen et al. investigated free and forced vibration analysis of the FG porous beams based on the Timoshenko beam theory. They obtained the natural frequencies of the beams subjected to different loading conditions and discussed different effects on the dynamic behavior of the FG porous beams [19]. In another attempt, Pagani and Carrera surveyed large displacements and post-buckling responses of composite beams based on the Carrera Unified Formulation. They used low to higher order beam theories to achieve the governing nonlinear equations of the beam [20]. In 2017, Wang and Zu investigated vibration behaviors of FG rectangular plates with even and uneven porosity distributions and moving in thermal condition. Vibration properties were presented, and the impact of some main parameters on the vibration behavior of the plates were analyzed [21]. Furthermore, in 2017, Wang and Zu studied the nonlinear steady-state response of FG plates. The plates were in contact with ideal liquid. The impact of some main parameters such as natural frequencies on the plates and different parameters on dynamic response of the plates were discussed [22]. In most recent attempt, in 2018, Nakhaei et al. presented a general formulation for the beam with crack by including crack parameters in the equation of motion. They determined the amplitude and frequency of the beam with circular and V-shapes cracks in their work [23]. Wang investigated electro-mechanical vibration analysis of FG plates with porosities in translation direction. The results have shown that the vibration properties of the plates relied on different physical parameters [24]. In another paper, Navabian et al. presented a novel damage index for the damage detection of plates based on mode shapes. The proposed damage index was capable of determining the location and severity of damage with high accuracy [25]. Furthermore, in 2018, Mottaghian et al. examined the vibration and statics response of cracked beams and bars based on the extended FE model. They determined the effects of different crack locations and boundary conditions on the stress counters and the displacement in their work [26]. In 2019, Soncco et al. studied the bending behavior of the FG beams based on the finite element method. The beams were under buckling loads and modeled based on an improved first-order shear deformation theory. They showed that the combination of ceramic and metal significantly affect the transverse deflections [27]. Mottaghian et al. investigated the large deformation response of cracked beams based on a new finite element model and continuum and classical-based methods [28]. In another work, Wang et al surveyed nonlinear vibration analysis of reinforced metal foam cylindrical shells based on Donnell nonlinear shell theory. Graphene platelets were utilized to

reinforce the shells. The impact of geometry properties of graphene platelets on vibration properties of the shells were investigated [29]. In 2020, Li et al investigated free vibration of FG beam immersed in fluid. Numerical results were performed to analyze the effect of different parameters such as fluid density on the vibration properties of the FG beam [30]. In another attempt, Wang et al studied free and forced vibration analysis of FG graphene oxide-reinforced beam based on a new Ritz-solution shape function. The beam was polymer nanocomposite and subjected to a moving load. An analysis was performed to demonstrate the impact of different parameters such as graphene oxide distribution on the response of FG beam with different boundary conditions [31]. In 2021, Salmalian et al. utilized a Lagrange multiplier approach within the nonlinear FE model to examine the cracked columns. The post-buckling responses of cracked FG columns subjected to thermal and mechanical loads were used to analyze the results. [32]. As can be seen, few works have been conducted on modeling of the damaged parts in functionally graded beams using springs; therefore, in this paper, an analytical method is provided for obtaining modal shapes and determining the location of damage for a functionally graded beam. The technique has a mathematical basis that is implemented on the Maple software. To show the accuracy and efficiency of the proposed method, the obtained frequencies are compared with the results presented in literature. The comparison indicates that the results are accurate, and the location of the damage was well illustrated in the diagram.

The paper is organized as follows: In the next section, the governing equations of the beam are extracted based on the first-order shear deformation theory. After that, the equations of the springs are presented, which are used to model the damaged elements. Thereafter, the continuity conditions, boundary conditions, and the solution for the governing equations of the beam are presented, respectively. Validation of the proposed method is performed in section 6. In section 7, the results of the models are shown and discussed. At the end, some conclusions are presented that can be used for further researches.

2 GOVERNING EQUATIONS OF THE BEAM

In this section, the governing equations of the beam are presented. The analyzed beam is divided to different parts (i.e., three parts) with different stiffness or different Young's modulus. E_1, E_2 and E_3 are the Young's modulus of part 1, 2 and 3, respectively (Fig.1). If the three parts of the beam are the same, same properties are considered for the parts.

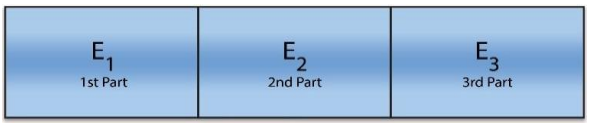

Fig.1
General model of the studied beam with three different parts.

To extract the governing equations, the first-order shear deformation theory is used, which is based on the displacement functions [33]:

$$u = u_0 + z\psi_x \qquad -\frac{h}{2} \le z \le \frac{h}{2} \tag{1}$$

where u is the in-plane displacement, u_0 is the in-plane displacement of the middle layer, ψ_x is the rotation of the transverse surface, and h is the thickness of the beam.

The governing equations of the beam can be extracted as follows:

$$\delta(U+K)=0 \tag{2}$$

where U is the internal energy, and K is the kinetic energy. The components of Eq. (2) are as follows:

$$\begin{aligned} \delta U &= \int_l \int_{-\frac{h}{2}}^{\frac{h}{2}} (\sigma_x \delta\varepsilon_x + \tau_{xz}\delta\gamma_{xz})dzdx \\ \delta K &= -\int_l \int_{-\frac{h}{2}}^{\frac{h}{2}} (\rho\ddot{u}\delta u + \rho\ddot{w}\delta w)dzdx \end{aligned} \tag{3}$$

where ε is the strain component, ρ is mass density, γ is shear strain, τ is shear stress, w is the displacement of the beam, X'' represents the second derivative of the function X based on the time and

$$\begin{aligned} &\sigma_x = \frac{E}{1-\nu^2}\varepsilon_x, \qquad \varepsilon_x = u_{,x} \\ &\tau_{xz} = k^2 \frac{E}{2(1+\nu)}\gamma_{xz}, \qquad \gamma_{xz} = u_{,z} + w_{,x} \end{aligned} \tag{4}$$

where k^2 is the transverse shear correction factor, which is used in first-order shear deformation theory. In this paper, $k^2 = 5/6$.

Substituting Eq. (1) and Eq. (4) into Eq. (3), gives Eq. (2) as follows:

$$\begin{aligned} &\int_l \int_{-\frac{h}{2}}^{\frac{h}{2}} [(\frac{E}{1-\nu^2} u_{0,x})\delta(u_{0,x} + z\psi_{x,x}) + (k^2 \frac{E}{2(1+\nu)})(\psi_x + w_{,x})\delta(\psi_x + w_{,x})]dzdx \\ &-\int_l \int_{-\frac{h}{2}}^{\frac{h}{2}} [\rho(\ddot{u}_0 + z\ddot{\psi}_x)\delta(u_0 + z\psi_x) + \rho\ddot{w}\,\delta w]dzdx \end{aligned} \tag{5}$$

Now the following equations can be defined for each part of the beam:

$$\begin{Bmatrix} A^{(s)} \\ B^{(s)} \\ D^{(s)} \end{Bmatrix} = \int_{-\frac{h}{2}}^{\frac{h}{2}} \frac{E^{(s)}}{1-\nu^{2(s)}} \begin{Bmatrix} 1 \\ z \\ z^2 \end{Bmatrix} dz \quad , \quad \overline{A}^{(s)} = \int_{-\frac{h}{2}}^{\frac{h}{2}} \frac{E^{(s)}}{2(1+\nu^{(s)})} dz \quad , \quad \begin{Bmatrix} I_0^{(s)} \\ I_1^{(s)} \\ I_2^{(s)} \end{Bmatrix} = \int_{-\frac{h}{2}}^{\frac{h}{2}} \rho^{(s)} \begin{Bmatrix} 1 \\ z \\ z^2 \end{Bmatrix} dz \tag{6}$$

where, s is the number of the desired element of the beam, and v is Poisson's ratio. Substituting Eq. (6) into Eq. (5), gives Eq. (2) and then integrating from that, the governing equations of the beam are extracted:

$$\begin{aligned} &A^{(s)} u_{0,xx}{}^{(s)} + B^{(s)} \psi_{x,xx}{}^{(s)} = I_0{}^{(s)} \ddot{u}_0{}^{(s)} + I_1{}^{(s)} \ddot{\psi}_x{}^{(s)} \\ &B^{(s)} u_{0,xx}{}^{(s)} + D^{(s)} \psi_{x,xx}{}^{(s)} - \overline{A}^{(s)} (\psi_x{}^{(s)} + w_{,x}{}^{(s)}) = I_1{}^{(s)} \ddot{u}_0{}^{(s)} + I_2{}^{(s)} \ddot{\psi}_x{}^{(s)} \\ &\overline{A}^{(s)} (\psi_{x,x}{}^{(s)} + w_{,xx}{}^{(s)}) = I_0{}^{(s)} \ddot{w}^{(s)} \end{aligned} \tag{7}$$

As one of the goals of this paper is the damage identification in the beam, in the next section, the damaged part is modeled with springs.

3 THE PROPOSED MODELS FOR THE SPRINGS

The damaged parts of the structure could be modeled by various methods: reducing the elasticity modulus, reducing the thickness of the damaged parts, using some springs, etc. To investigate the damage beams, two general techniques are considered in this study:

1. Analysis of the damaged beam with real elements and different modulus of elasticity (as shown in Fig. 1)
2. Analysis of the damaged beam with two new presented spring-based models:

- Modeling the damaged element of the beam with longitudinal continuous springs with stiffnesses k_u. (as shown in Fig. 2(a)). For the case of FG beams, k_u is changed along the thickness direction.
- Modeling the damaged element of the beam with equivalent longitudinal and rotational springs with stiffnesses $\overline{k_u}$ and k_ϕ. (as shown in Fig. 2(b)).

Fig.2 illustrates the overall process of damage identification based on the two presented springs models.

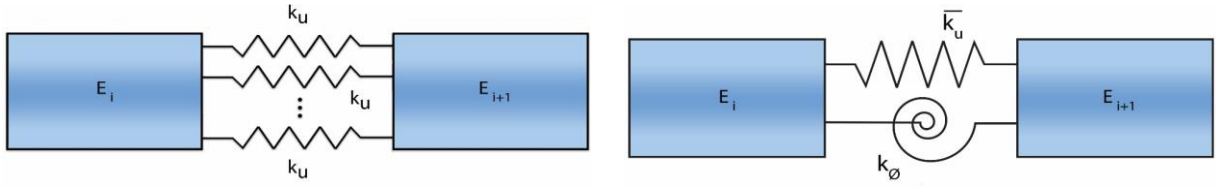

Fig.2
Modeling the damaged element based on: a) longitudinal continuous springs and b) equivalent longitudinal and rotational springs.

In this section, the equations of the springs for homogeneous, functionally graded materials (FGM), and equivalent conditions are discussed. Modeling the parts by springs results in lower time consuming of the calculation process.

3.1 Proposed model of springs for homogeneous beam

The stiffnesses of the springs when the modulus of elasticity is constant along the thickness of the beam are extracted as follows:

$$N_x = \int_{-\frac{h_d}{2}}^{\frac{h_d}{2}} \sigma_x dz = \int_{-\frac{h_d}{2}}^{\frac{h_d}{2}} k_u \Delta u dz \tag{8}$$

$$M_x = \int_{-\frac{h_d}{2}}^{\frac{h_d}{2}} \sigma_x z dz = \int_{-\frac{h_d}{2}}^{\frac{h_d}{2}} k_u \Delta u z dz \tag{9}$$

where the index *d* refers to the damaged element of the beam, which modeled by springs, σ_x is expressed in Eq. (4), and in this section, the strain component and Δu which is the displacement of the longitudinal springs can be defined as follows:

$$\begin{aligned} &\varepsilon_x = \frac{\Delta u}{x_d} \\ &\Delta u = (u_0^{(i)} + z\psi_x^{(i)}) - (u_0^{(i+1)} + z\psi_x^{(i+1)}) \end{aligned} \tag{10}$$

where x_d is the length of the damaged element of the beam. By substituting σ_x and Eq. (10) into Eq. (8) and Eq. (9), gives the following equations:

$$\int_{-\frac{h_d}{2}}^{\frac{h_d}{2}} \frac{E_d}{1-\nu_d^2} \frac{\Delta u}{x_d} dz = \int_{-\frac{h_d}{2}}^{\frac{h_d}{2}} k_u \Delta u dz \tag{11}$$

$$\int_{-\frac{h}{2}}^{\frac{h}{2}} \frac{E_d}{1-\nu_d^2} \frac{\Delta u}{x_d} z dz = \int_{-\frac{h}{2}}^{\frac{h}{2}} k_u \Delta u z dz \tag{12}$$

k_u results from the above equations as follows:

$$k_u = \frac{E_d}{(1-\nu_d{}^2)x_d} \tag{13}$$

In this section, for a homogeneous beam, the longitudinal springs can be equivalenced with a longitudinal and rotational springs ($\overline{k_u}$ and k_ϕ in Fig.2, respectively). Therefore

$$N_x = \overline{k_u}\Delta u_0 \tag{14}$$

$$M_x = k_\phi \Delta\phi \tag{15}$$

By substituting σ_x and Eq. (10) into Eq. (14) and Eq. (15), gives the following equations:

$$\int_{-\frac{h_d}{2}}^{\frac{h_d}{2}} \frac{E_d}{1-\nu_d{}^2}\frac{\Delta u_0}{x_d}dz = \overline{k_u}\Delta u_0 \tag{16}$$

$$\int_{-\frac{h_d}{2}}^{\frac{h_d}{2}} \frac{E_d}{1-\nu_d{}^2}\frac{\Delta u_0}{x_d}z dz = k_\phi \Delta\phi \tag{17}$$

Therefore, the stiffnesses of the longitudinal and rotational springs in this section will be:

$$\overline{k_u} = \frac{E_d h_d}{(1-\nu_d{}^2)x_d} \quad , \quad k_\phi = \frac{E_d h_d{}^3}{12(1-\nu_d{}^2)} = \frac{h_d{}^2}{12}\overline{k_u} \tag{18}$$

3.2 Proposed model of springs for the FG beam

If the modulus of elasticity is a function of z , Eq. (18) is not applicable. In this case, the calculations should be done in integral form for the boundary conditions, and k_u consists of two parameters as follows:

$$k_u = k_{u_0} + z k_{u_1} \tag{19}$$

Therefore, the stiffnesses of the proposed springs for the FG beam are extracted as follows:

$$N_x = \int_{-\frac{h_d}{2}}^{\frac{h_d}{2}} \sigma_x dz = \int_{-\frac{h_d}{2}}^{\frac{h_d}{2}} k_u \Delta u dz \tag{20}$$

$$M_x = \int_{-\frac{h_d}{2}}^{\frac{h_d}{2}} \sigma_x z dz = \int_{-\frac{h_d}{2}}^{\frac{h_d}{2}} k_u \Delta u z dz \tag{21}$$

By substituting σ_x and strain component into Eq. (20) and Eq. (21), the following equations result:

$$\int_{-\frac{h_d}{2}}^{\frac{h_d}{2}} \frac{E_d(z)}{1-\nu_d{}^2}\frac{\Delta u}{x_d}dz = \int_{-\frac{h_d}{2}}^{\frac{h_d}{2}} (k_{u_0}+zk_{u_1})\Delta u dz \tag{22}$$

$$\int_{-\frac{h_d}{2}}^{\frac{h_d}{2}} \frac{E_d(z)}{1-\nu_d{}^2}\frac{\Delta u}{x_d}zdz = \int_{-\frac{h_d}{2}}^{\frac{h_d}{2}} (k_{u_0}+zk_{u_1})\Delta u z dz \tag{23}$$

Therefore, the stiffness of the springs will be:

$$k_{u_0} = \int_{-\frac{h_d}{2}}^{\frac{h_d}{2}} \frac{E_d}{h_d(1-\nu_d{}^2)x_d}dz \quad , \quad k_{u_1} = \int_{-\frac{h_d}{2}}^{\frac{h_d}{2}} \frac{12E_d}{h_d{}^3(1-\nu_d{}^2)x_d}zdz \tag{24}$$

3.3 Proposed equivalent springs for the FG and homogeneous beam

We considered an equivalent condition for the stiffnesses of the springs that could be expressed for both homogeneous and FGM beams. The equivalent stiffnesses of the springs are as follows:

$$k_u = \int_{-\frac{h_d}{2}}^{\frac{h_d}{2}} \frac{E_d(z)}{(1-\nu_d{}^2)x_d}dz \quad , \quad k_\varphi = \int_{-\frac{h_d}{2}}^{\frac{h_d}{2}} \frac{E_d(z)\times z^2}{(1-\nu_d{}^2)x_d}dz \tag{25}$$

In fact, if the elasticity modulus is not a function of z, the above equation will be the same as Eq. (18). By modeling one part of the beam with springs as above, one element of the beam is eliminated, and the natural frequencies of the beam are calculated with high precision and fewer computation costs.

4 CONTINUITY CONDITIONS OF THE BEAM

In this section, the continuity conditions of displacements and different boundary conditions which are applied to model the beam are presented.

4.1 Continuity conditions of the beam

In this section, the continuity conditions of the beam for the two models, which are considered to investigate the damage in this study, are presented. The continuity conditions of displacements and stress resultants must be established between different elements of the beam. In this beam, the length of the first, second, and third elements are x_1, x_2, and x_3, respectively.

For the model of the beam with real elements and modulus of elasticity, the continuity conditions are expressed as follows:

$$x = x_1 \rightarrow \begin{cases} u_0^{(1)} = u_0^{(2)} \\ \psi_x^{(1)} = \psi_x^{(2)} \\ w^{(1)} = w^{(2)} \\ N_x^{(1)} = N_x^{(2)} \\ M_x^{(1)} = M_x^{(2)} \\ Q_x^{(1)} = Q_x^{(2)} \end{cases} , \quad x = x_1 + x_2 \rightarrow \begin{cases} u_0^{(2)} = u_0^{(3)} \\ \psi_x^{(2)} = \psi_x^{(3)} \\ w^{(2)} = w^{(3)} \\ N_x^{(2)} = N_x^{(3)} \\ M_x^{(2)} = M_x^{(3)} \\ Q_x^{(2)} = Q_x^{(3)} \end{cases} \tag{26}$$

where N_x , M_x , and Q_x are the in-plane force, the bending torque, and the transverse shear force per unit length, respectively and are defined through the first-order shear deformation theory:

$$\begin{aligned} N_x{}^{(s)} &= A^{(s)} u_{0,x}{}^{(s)} + B^{(s)} \psi_{x,x}{}^{(s)} \\ M_x{}^{(s)} &= B^{(s)} u_{0,x}{}^{(s)} + D^{(s)} \psi_{x,x}{}^{(s)} \\ Q_x{}^{(s)} &= \overline{A}^{(s)} (\psi_x{}^{(s)} + w_{,x}{}^{(s)}) \end{aligned} \tag{27}$$

For the elements of the beam connected with springs, the continuity conditions of displacements and stress resultants must be established between elements and springs, and these conditions are as follows:

The continuity conditions for the FGM are:

$$\begin{cases} x = \dfrac{x_1 + x_2}{2} \rightarrow \displaystyle\int_{-\frac{h}{2}}^{\frac{h}{2}} k_u (u^{(i)} - u^{(i+1)}) dz = N_x{}^{(i)} = N_x{}^{(i+1)} \\ x = \dfrac{x_1 + x_2}{2} \rightarrow \displaystyle\int_{-\frac{h}{2}}^{\frac{h}{2}} k_u (u^{(i)} - u^{(i+1)}) z dz = M_x{}^{(i)} = M_x{}^{(i+1)} \end{cases} , \begin{cases} x = \dfrac{x_1 + x_2}{2} \rightarrow w^{(i)} = w^{(i+1)} \\ x = \dfrac{x_1 + x_2}{2} \rightarrow Q_x{}^{(i)} = Q_x{}^{(i+1)} \end{cases} \tag{28}$$

and the continuity conditions for the homogeneous and equivalent condition are:

$$\begin{cases} x = \dfrac{x_1 + x_2}{2} \rightarrow \displaystyle\int_{-\frac{h}{2}}^{\frac{h}{2}} k_u (u^{(i)} - u^{(i+1)}) dz = N_x{}^{(i)} = N_x{}^{(i+1)} \\ x = \dfrac{x_1 + x_2}{2} \rightarrow \displaystyle\int_{-\frac{h}{2}}^{\frac{h}{2}} k_\phi (\psi_x{}^{(i)} - \psi_x{}^{(i+1)}) dz = M_x{}^{(i)} = M_x{}^{(i+1)} \end{cases} , \begin{cases} x = \dfrac{x_1 + x_2}{2} \rightarrow w^{(i)} = w^{(i+1)} \\ x = \dfrac{x_1 + x_2}{2} \rightarrow Q_x{}^{(i)} = Q_x{}^{(i+1)} \end{cases} \tag{29}$$

4.2 Boundary conditions

The following boundary conditions are considered for various support conditions:

Clamped edge:

$$\begin{cases} u_0 = 0 \\ \psi_x = 0 \\ w = 0 \end{cases} \tag{30}$$

Simply-supported edge:

$$\begin{cases} u_0 = 0 \\ M_x = 0 \\ w = 0 \end{cases} \tag{31}$$

Free edge:

$$\begin{cases} M_x = 0 \\ N_x = 0 \\ Q_x = 0 \end{cases} \tag{32}$$

5 THE SOLUTION OF GOVERNING EQUATIONS OF THE BEAM WITH POWER SERIES

To achieve the displacement components, the governing equations must be solved; therefore, by using power series method based on Taylor's series expansion, the functions can be expressed by the following power series whose centers are located at $x=m$. N is the number of statements of the power series which is achieved through a sensitivity analysis for a convergent result.

$$\begin{cases} u_0 = \sum_{i=0}^{N} U_i (x-m)^i = U_0 + U_1(x-m) + U_2(x-m)^2 + \dots \\ \psi_x = \sum_{i=0}^{N} \phi_i (x-m)^i = \phi_0 + \phi_1(x-m) + \phi_2(x-m)^2 + \dots \\ w = \sum_{i=0}^{N} W_i (x-m)^i = W_0 + W_1(x-m) + W_2(x-m)^2 + \dots \end{cases} \tag{33}$$

5.1 The Solution of governing beam equations

For the first beam element, the power series expand around the m = 0, and for the other elements of the beam, the power series expands around the end length of the previous element. Substituting Eq. (33) into Eq. (7), the following three equations of the beam are obtained:

$$\begin{aligned} &\sum_{i=0}^{N} [A^{(s)}(i+2)(i+1)U_{i+2}^{(s)} + B^{(s)}(i+2)(i+1)\phi_{i+2}^{(s)} + I_0^{(s)}\omega^2 U_i^{(s)} + I_1^{(s)}\omega^2 \phi_i^{(s)}]x^i = 0 \\ &\sum_{i=0}^{N} [B^{(s)}(i+2)(i+1)U_{i+2}^{(s)} + D^{(s)}(i+2)(i+1)\phi_{i+2}^{(s)} - \overline{A}^{(s)}(\phi_i^{(s)} + (i+1)W_{i+1}^{(s)}) + I_1^{(s)}\omega^2 U_i^{(s)} + I_2^{(s)}\omega^2 \phi_i^{(s)}]x^i = 0 \\ &\sum_{i=0}^{N} [\overline{A}^{(s)}(i+1)\phi_{i+1}^{(s)} + \overline{A}^{(s)}(i+2)(i+1)W_{i+2}^{(s)} + I_0^{(s)}\omega^2 W_i^{(s)}]x^i = 0 \end{aligned} \tag{34}$$

5.2 Transformation of the beam boundary conditions

In this section, we put the power series into the boundary conditions as follows:

Clamped edge:

$$\begin{cases} U_0 = 0 \\ \phi_0 = 0 \\ W_0 = 0 \end{cases} \tag{35}$$

Simply-supported edge:

$$\begin{cases} U_0 = 0 \\ BU_1 + D\phi_1 = 0 \\ W_0 = 0 \end{cases} \tag{36}$$

Free edge:

$$\begin{cases} BU_1 + D\phi_1 = 0 \\ AU_1 + B\phi_1 = 0 \\ \overline{A}(\phi_0 + W_1) = 0 \end{cases} \tag{37}$$

By solving the governing equations of the beam, $U_j^{(i)}$, $\phi_j^{(i)}$, $W_j^{(i)}$ with j =2.3 ….n are achieved according to $U_0^{(i)}, U_1^{(i)}$, $\phi_0^{(i)}, \phi_1^{(i)}$, $W_0^{(i)}$, $W_1^{(i)}$. Therefore, the equation of the beam based on continuity and boundary conditions can be shown as the following matrix equation:

$$\begin{bmatrix} X_{11}(\omega) & \cdots & X_{1n}(\omega) \\ X_{21}(\omega) & \cdots & X_{2n}(\omega) \\ X_{31}(\omega) & \cdots & X_{3n}(\omega) \\ \vdots & \ddots & \vdots \\ X_{(n-1)1}(\omega) & \cdots & X_{(n-1)n}(\omega) \\ X_{n1}(\omega) & \cdots & X_{n1}(\omega) \end{bmatrix} \times \begin{Bmatrix} U_1^{(1)} \\ \phi_1^{(1)} \\ W_1^{(1)} \\ \vdots \\ \phi_3^{(1)} \\ W_3^{(1)} \end{Bmatrix} = \begin{Bmatrix} 0 \\ 0 \\ 0 \\ \vdots \\ 0 \\ 0 \end{Bmatrix} \tag{38}$$

where $X_{ij}(\omega)$ is the *ith* row and *jth* column of the matrix that is expressed based on the natural frequency of the beam.

6 VALIDATION OF THE PROPOSED METHOD

In this section, validation of the proposed method and results of natural frequencies are provided. To validate the accuracy of the proposed method, the results are compared with those of literature [12]. Table 1 shows the analytical results of the first three natural frequencies and compared with CBT and TBT methods for the functionally graded beam. In this table, C-C, S-S, and F-F are related to boundary conditions and denotes for clamped-clamped, simply supported-simply supported, and free-free conditions, respectively. The functionally graded materials are mixtures of Aluminium and Alumina (Al_2O_3), which their properties are as follows:

$$\begin{aligned} &\text{Aluminium: } E = 70Gpa,\ \nu = 0.3,\ \ \rho = 2700\frac{kg}{m^3} \\ &\text{Alumina: } E = 380Gpa,\ \nu = 0.3,\ \ \rho = 3800\frac{kg}{m^3} \end{aligned} \tag{39}$$

The power-law variation, which is used in this section and Ref. [12] is considered as follows:

$$R(z) = (R_c - R_m)(\frac{z}{h} + \frac{1}{2})^k + R_m \tag{40}$$

where R_c and R_m denote the values of the properties of the Alumina and Aluminum constituents of the FG beam, respectively, and k is the power-law indices. It is important to note that the non-dimensional frequency parameter, which is used in this paper, is expressed as follows:

$$\omega = \frac{\lambda L^2}{h}\sqrt{\frac{\rho_m}{E_m}} \tag{41}$$

where λ is the achieved frequency, L is the length of the beam, h is the thickness of the beam, and ρ_m and E_m are the mass density and Young's modulus of the Aluminum, respectively.

Table 1
The first three natural frequencies of the beam with fixed L/h = 5 and different power-law indices (k).

BC's	Natural frequency	K=2			K=5			K=10		
		CBT [12]	TBT [12]	This Study	CBT [12]	TBT [12]	This Study	CBT [12]	TBT [12]	This Study
C-C	ω_1	9.6297	8.1436	7.6940	8.8444	7.2733	7.0954	8.4517	6.7977	6.7405
	ω_2	24.4029	17.6106	17.8762	21.4108	15.4037	16.2161	19.5030	14.2226	15.2798
	ω_3	26.6125	25.8414	24.2027	23.3156	21.6583	20.9120	22.1017	19.5473	19.1003
S-S	ω_1	4.7519	4.5239	3.854	4.3132	4.0732	3.6266	3.9598	3.7305	3.4970
	ω_2	15.2414	13.3481	13.5587	13.8836	11.9338	12.5735	13.5466	11.2966	12.025
	ω_3	23.3528	23.3498	24.1871	22.4586	20.3628	20.8812	20.1299	18.7676	19.0744

F-F	ω_1	8.9226	8.4635	8.1467	8.1944	7.6957	7.6452	7.8836	7.3316	7.3992
	ω_2	22.3792	18.4173	19.3040	20.5191	16.3610	17.8765	19.7413	15.3066	17.1655
	ω_3	26.3180	25.2117	24.2709	22.1065	21.3348	21.0023	19.8473	19.3327	19.1586

As can be seen, the results of the proposed method are closer to the TBT method, which indicates the high accuracy of the proposed method. Also, the good agreement between the results of this study and those of the literature, shows the convergence of the results for different conditions. Table 2 shows the achieved results for different statement numbers of the power series. The boundary condition and the power-law indices, *k*, are considered as C-C and 10, respectively. As can be seen the results converge to their final value, properly.

Table 2
The achieved results for different statement numbers of the power series (C-C boundary condition and *k*=10).

Natural frequency	*N*=20	*N* =25	*N* =30	*N* =35	*N* =40
ω_1	6.7405	6.7405	6.7405	6.7405	6.7405
ω_2	15.3377	15.2799	15.2798	15.2798	15.2798
ω_3	19.1002	19.1004	19.1003	19.1003	19.1003

7 RESULTS AND DISCUSSION

In this section, to show the accuracy of the proposed spring stiffness formulas, a comparison is made between the first three natural frequencies of the beams, which contain parts that are modeled by real elements and the ones which are modeled by the spring formulas extracted in section 3. These comparisons are made for undamaged and damaged beams and homogeneous and FGM conditions. For this purpose, a beam with three elements is considered, and the second element is modeled by the proposed springs; the results are compared with those of the real element modeling. The beam properties in this section are considered as follows:

$$E = (E_c - E_m)(\frac{z}{h} + \frac{1}{2})^k + E_m \quad , \quad \rho = (\rho_c - \rho_m)(\frac{z}{h} + \frac{1}{2})^k + \rho_m$$
$$E_c = 70Gpa \quad , \quad E_m = 380Gpa \quad , \quad \rho_c = 2700\,{kg}/{m^3} \quad , \quad \rho_m = 3800\,{kg}/{m^3} \tag{42}$$
$$\nu = 0.3 \quad , L = 1 \quad , \quad h = 0.2$$

Table 3 shows the comparison for an undamaged clamped-clamped beam, which is modeled by real elements, spring (section 3.1 and 3.2), and equivalent spring (section3.3). Different spring lengths are considered, and the material is assumed homogeneous ($k = 0$) and FGM. The whole length of the beam is unit; the first element length is assumed as 0.5, and the spring length is defined in the table.

Table 3
Comparison of the three first non-dimensional frequencies of the undamaged clamped-clamped beam with different modeling conditions.

Spring length	Natural frequency	*k* = 0			*K* = 2			*K* = 5		
		E	Spring	Equivalent spring	E	Spring	Equivalent spring	E	Spring	Equivalent spring
0.001	ω_1	5.5230	5.5202	5.5202	9.0753	9.0564	9.0707	9.7598	9.7467	9.7547
	ω_2	12.7348	12.7348	12.7348	21.2374	21.2377	21.2375	22.8051	22.8052	22.8051
	ω_3	16.4664	16.4664	16.4664	28.9880	28.988	28.988	30.7988	30.7987	30.7987
0.01	ω_1	5.5230	5.4956	5.4956	9.0753	8.8996	9.0288	9.7598	9.6348	9.7086
	ω_2	12.7348	12.7347	12.7347	21.2374	21.2604	21.2405	22.8051	22.8190	22.8068
	ω_3	16.4664	16.4664	16.4664	28.9880	28.9839	28.9834	30.7988	30.7962	30.7961
0.05	ω_1	5.5230	5.3965	5.3965	9.0753	8.3994	8.8417	9.7598	9.2408	9.5109
	ω_2	12.7348	12.7235	12.7235	21.2374	21.5260	21.2883	22.8051	22.9938	22.8257
	ω_3	16.4664	16.4613	16.4613	28.9880	28.9001	28.883	30.7988	30.744	30.7376

0.1	ω_1	5.5230	5.2996	5.2996	9.0753	8.0344	8.6309	9.7598	8.9176	9.2993
	ω_2	12.7348	12.6541	12.6541	21.2374	21.7219	21.2972	22.8051	23.1047	22.7712
	ω_3	16.4664	16.4264	16.4264	28.9880	28.6922	28.6298	30.7988	30.6041	30.5784

As can be seen, the results of the proposed spring formulations are in good agreement with the real one in the undamaged beam. In all the tables presented in this section, for $k = 0$, since the equation of equivalent spring is coincided with equation of spring in homogeneous condition, the natural frequencies presented for them are the same.

To study the applicability of the proposed spring formulation in damaged beams, a 30 percent reduction in elasticity modulus is applied on the second element of the previous beam, and the comparisons are shown in Table 4. The first element length is considered as 0.2.

Table 4
Comparison of the first three non-dimensional frequencies of the damaged clamped-clamped beam with different modeling conditions.

Damaged length	Natural frequency	$k = 0$			$K = 2$			$K = 5$		
		E	Spring	Equivalent spring	E	Spring	Equivalent spring	E	Spring	Equivalent spring
0.001	ω_1	5.5224	5.5229	5.5229	9.0746	9.0776	9.0752	9.759	9.7611	9.7597
	ω_2	12.7325	12.7306	12.7306	21.2337	21.2305	21.2313	22.8011	22.7981	22.7978
	ω_3	16.4618	16.4510	16.4510	28.98	28.9612	28.9579	30.7902	30.7701	30.7687
0.01	ω_1	5.5179	5.5216	5.5216	9.068	9.1011	9.0744	9.7517	9.7743	9.7581
	ω_2	12.7123	12.6972	12.6972	21.1999	21.1696	21.1811	22.7649	22.7389	22.7390
	ω_3	16.4216	16.3124	16.3124	28.9098	28.7232	28.6788	30.7152	30.5139	30.4925
0.05	ω_1	5.5	5.5039	5.5039	9.0423	9.2463	9.0640	9.7234	9.8542	9.7376
	ω_2	12.6177	12.6311	12.6311	21.0363	20.9364	21.0474	22.5910	22.5485	22.6038
	ω_3	16.2689	15.7026	15.7026	28.6433	27.7422	27.3763	30.4304	29.4316	29.2122
0.1	ω_1	5.4769	5.4452	5.4452	9.0074	9.4795	9.0269	9.6852	9.9617	9.6687
	ω_2	12.4966	12.6715	12.6715	20.8190	21.6638	21.3896	22.3616	23.0322	22.8441
	ω_3	16.1341	14.9747	14.9747	28.4073	26.1445	25.7868	30.1788	27.8619	27.6748

The results of Table 4 demonstrate the applicability of the proposed spring formulation in the presence of the damage. Considering the accuracy of the proposed numerical method, which is shown previously, any reduction in the natural frequency indicates the presence of damage in the structure. To identify the damaged location through a nondestructive process, many approaches have been proposed. Using mode shape derivatives is one of the useful nondestructive techniques. Studies have shown that the mode shape derivatives, especially the second derivative of mode shapes, are sensitive parameters that show the location of damage in the structure ([34, 35]). To display the applicability of the proposed numerical method in locating the damaged parts of the beam, a clamped-clamped FG beam is considered. The whole length of the beam is unit, the first element length is 0.5, and the second element is considered as the damaged element. The damaged element length is assumed as 0.05, and a 30 percent reduction in its elasticity modulus is considered.

Table 5 compares the first three non-dimensional frequencies of the above-mentioned beam with those of undamaged one. In Fig.3, the second derivative of the mode shape of the above-mentioned damaged beam is shown. As can be seen, the graph shows a discontinuity in the location of the second element. No discontinuity is seen in other parts of the beam that is adopted to the primary assumption.

Table 5
Comparison of the first three non-dimensional frequencies of the undamaged and damaged FGM C-C beam.

Natural frequency	K=2 Undamaged beam			K=2 Damaged beam		
	E	Spring	Equivalent spring	E	Spring	Equivalent spring
ω_1	9.0753	8.3994	8.8417	8.9765	8.2074	8.7405
ω_2	21.2374	21.5260	21.2883	21.1417	21.5078	21.2778
ω_3	28.9880	28.9001	28.883	28.9769	28.8612	28.8253

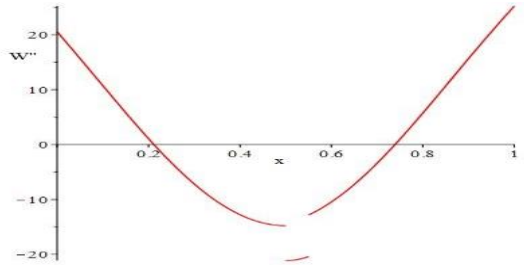

Fig.3
Damage localization result for C-C Beam.

In the following, instead of applying the damage in elasticity modulus, the thickness of the beam in the second element is reduced to 50 percent of its primary value. Table 6. shows the frequency results for different modeling methods. As can be seen, there is a good agreement between the natural frequencies results for the case of element thickness reduction. As could be seen, the proposed springs can properly model the thickness reduction in the damaged elements with different lengths.

Table 6
Comparison of the first three non-dimensional frequencies of the C-C beam with 50 percent thickness reduction in the second element.

Damaged length	Natural frequency	*k*=0			*k*=2			*k*=5		
		E	Spring	Equivalent spring	E	Spring	Equivalent spring	E	Spring	Equivalent spring
0.001	ω_1	5.507	5.5010	5.5010	9.0471	9.0617	9.0144	9.7298	9.7496	9.6951
	ω_2	12.7329	12.7348	12.7348	21.2351	21.2376	21.2375	22.8023	22.8051	22.8051
	ω_3	16.4746	16.4664	16.4664	29.0020	28.9879	28.9878	30.8140	30.7987	30.7987
0.01	ω_1	5.3816	5.3261	5.3261	8.8273	8.9431	8.7854	9.4955	9.6592	9.4555
	ω_2	12.7154	12.7341	12.7341	21.2131	21.2515	21.2442	22.7760	22.8113	22.8085
	ω_3	16.5491	16.4663	16.4663	29.1287	28.9797	28.9792	30.9517	30.7939	30.7938
0.05	ω_1	5.0922	4.8607	4.8607	8.3273	8.5001	7.9715	8.9581	9.2982	8.6264
	ω_2	12.5851	12.6728	12.6728	21.0180	21.4502	21.3682	22.5566	22.8964	22.8403
	ω_3	16.8796	16.4563	16.4563	29.6871	29.7797	28.7463	31.5615	30.6820	30.6664
0.1	ω_1	5.0335	4.7111	4.7111	8.2265	7.8026	7.6049	8.8463	8.5000	8.2342
	ω_2	12.2883	12.0453	12.0453	20.5153	20.8693	20.5037	22.0111	22.2068	21.8595
	ω_3	17.2551	17.3017	17.3017	30.3126	29.6265	29.5948	32.2513	32.0432	32.0290

To show the efficiency of the proposed numerical method for the other boundary conditions, two new boundary conditions (simply supported-simply supported and free-free conditions) are applied on the beam. In Table 7, the damage is considered on the second element, with a 30 percent reduction in the elasticity modulus. The whole length of the beam is unit, the first element length is 0.5, and the second element length is 0.001.

Table 7
Comparison of the first three natural frequencies with various modeling method and different boundary conditions.

B. C's	Natural frequency	*k*=0			*k*=2			*k*=5		
		E	Spring	Equivalent spring	E	Spring	Equivalent spring	E	Spring	Equivalent spring
S-S	ω_1	2.8158	2.8132	2.8132	4.5288	4.509	4.5250	4.8885	4.8750	4.8841
	ω_2	9.8390	9.8401	9.8401	16.0427	16.0442	16.0441	17.2959	17.2975	17.2975
	ω_3	16.4594	16.4429	16.4429	28.9705	28.9587	28.9559	30.7834	30.7624	30.7618
F-F	ω_1	6.0109	6.0041	6.0041	9.6531	9.7011	9.6486	10.4455	10.4715	10.4373
	ω_2	14.1473	14.1495	14.1495	23.0221	23.0226	23.0248	24.8847	24.8866	24.8879
	ω_3	16.4594	16.4429	16.4429	29.0003	28.7411	28.7628	30.7951	30.6388	30.6474

As seen in all the above tables, the frequencies are in very good agreement, which shows the applicability of the proposed numerical approaches in different boundary conditions. The above examples have been conducted for a

three-element beam that one of its elements has been damaged. To find a more exact location of the damaged zone, the element number could be increased. Also, for the case of multiple damaged elements, the number of springs can be increased. In the following, to show the applicability of the proposed method in locating the damaged parts of the beam, a clamped-clamped FG beam is considered. The beam is modeled by four parts, at which it's two middle parts are damaged which are modeled by two springs. The whole length of the beam is unit, the first element length is 0.5, and the whole length of the two springs is defined in Table 8, 20 percent reduction in elasticity modulus is considered in the damaged elements.

Table 8
Comparison of the first three non-dimensional frequencies of the damaged clamped-clamped beam with different damaged lengths.

Damaged length	Natural frequency	k=2		k=5	
		Spring	Equivalent spring	Spring	Equivalent spring
0.001	ω_1	9.0477	9.0656	9.7393	9.7488
	ω_2	21.5313	21.2313	22.7987	22.798
	ω_3	28.9846	28.984	30.7951	30.7949
0.01	ω_1	8.8217	8.9761	9.5650	9.6494
	ω_2	21.4161	21.1857	22.7696	22.7447
	ω_3	28.9548	28.9496	30.7657	30.7638
0.05	ω_1	8.1385	8.5714	8.9722	9.2204
	ω_2	21.3884	21.1552	22.6667	22.6908
	ω_3	28.8443	28.8365	30.6971	30.6928
0.1	ω_1	7.6974	8.1610	8.5333	8.8008
	ω_2	21.1343	21.0968	22.5773	22.6337
	ω_3	28.7905	28.8036	30.6732	30.6636

As can be seen, the results of the proposed springs and equivalent springs are in good agreement with each other when there are several damaged parts in the beam. In the following, for the abovementioned beam, instead of applying the damage in elasticity modulus, the thicknesses of the beam in the damaged elements are reduced to 50 percent of their primary values. Table 9 shows the frequency results for the case of element thickness reduction. As before, there is a good agreement between the natural frequencies results for the case of elements thickness reduction.

Table 9
Comparison of the first three non-dimensional frequencies of the damaged clamped-clamped beam with thickness reduction in the damaged elements.

Damaged length	Natural frequency	k=2		k=5	
		Spring	Equivalent spring	Spring	Equivalent spring
0.001	ω_1	9.0562	9.0229	9.7437	9.7039
	ω_2	21.229	21.2029	22.7959	22.7677
	ω_3	28.9823	28.9795	30.7932	30.7922
0.01	ω_1	8.8888	8.6080	9.6008	9.2657
	ω_2	21.1766	20.9452	22.7311	22.4971
	ω_3	28.9336	28.9133	30.7488	30.7421
0.05	ω_1	8.2665	7.5516	9.0339	8.1636
	ω_2	21.0176	20.5910	22.695	22.1075
	ω_3	28.7526	28.7134	30.6444	30.6336
0.1	ω_1	7.778	7.0428	8.5471	7.6264
	ω_2	21.0830	20.6179	22.6073	22.0963
	ω_3	28.5235	28.9463	30.5677	30.3843

8 CONCLUSION

In this paper, for the first time, an analytical method based on a new model of springs has been introduced, and is used to model the damaged elements of the beam. The proposed method can be applied for the analysis of structures with fewer computation costs and high accuracy. To show the accuracy of the proposed method, the natural frequencies of the beams with real elements and the ones which have been modeled by the proposed springs have been compared. The comparisons have been made for various support conditions, and good agreement between the results has been observed. In another attempt, to find the damaged part of the beam, the second derivative of the mode shapes has been surveyed. The location of discontinuity on the graph is a representation of the damaged part. The proposed method could be expanded to apply in real structures.

REFERENCES

[1] Rytter A., 1993, *Vibrational Based Inspection of Civil Engineering Structures*, *Ph.D. thesis,* Department of Building Technology and Structural Engineering, Aalborg University.

[2] Wu J.S., Huang C.G., 1995, Free and forced vibrations of a Timoshenko beam with any number of translational and rotationalsprings and lumped masses, *Communications in Numerical Methods in Engineering* **11**(9): 743-756.

[3] Chondros T., Dimarogonas A., Yao J., 1998, A continuous cracked beam vibration theory, *Journal of Sound and Vibration* **215**(1): 17-34.

[4] Li W.L., 2000, Free vibrations of beams with general boundary conditions, *Journal of Sound and Vibration* **237**(4): 709-725.

[5] Patil D., Maiti S., 2003, Detection of multiple cracks using frequency measurements, *Engineering Fracture Mechanics* **70**(12): 1553-1572.

[6] Lu C-F., Chen W., 2005, Free vibration of orthotropic functionally graded beams with various end conditions, *Structural Engineering and Mechanics* **20**(4): 465-476.

[7] Aydogdu M., Taskin V., 2007, Free vibration analysis of functionally graded beams with simply supported edges, *Materials & Design* **28**(5): 1651-1656.

[8] Sina S., Navazi H., Haddadpour H., 2009, An analytical method for free vibration analysis of functionally graded beams, *Materials & Design* **30**(3): 741-747.

[9] Şimşek M., 2010, Vibration analysis of a functionally graded beam under a moving mass by using different beam theories, *Composite Structures* **92**(4): 904-917.

[10] Moradi S., Razi P., Fatahi L., 2011, On the application of bees algorithm to the problem of crack detection of beam-type structures, *Computers & Structures* **89**(23-24): 2169-2175.

[11] Manoach E., Samborski S., Mitura A., Warminski J., 2012, Vibration based damage detection in composite beams under temperature variations using Poincaré maps, *International Journal of Mechanical Sciences* **62**(1): 120-132.

[12] Pradhan K., Chakraverty S., 2013, Free vibration of Euler and Timoshenko functionally graded beams by Rayleigh–Ritz method, *Composites Part B: Engineering* **51**: 175-184.

[13] Wattanasakulpong N., Ungbhakorn V., 2014, Linear and nonlinear vibration analysis of elastically restrained ends FGM beams with porosities, *Aerospace Science and Technology* **32**(1): 111-120.

[14] Shariyat M., Alipour M. M., 2011, Differential transform vibration and modal stress analyses of circular plates made of two-directional functionally graded materials resting on elastic foundations, *Archive of Applied Mechanics* **81**: 1289-1306.

[15] Shariyat M., Alipour M. M., 2013, A power series solution for vibration and complex modal stress analyses of variable thickness viscoelastic two-directional FGM circular plates on elastic foundations, *Applied Mathematical Modelling* **37**: 3063-3076.

[16] Alipour M. M., Shariyat M., 2010, Stress analysis of two-directional FGM moderately thick constrained circular plates with non-uniform load and substrate stiffness distributions, *Journal of Solid Mechanics* **2**: 316-331.

[17] Alipour M. M., Shariyat M., 2011, A power series solution for free vibration of variable thickness Mindlin circular plates with two-directional material heterogeneity and elastic foundations, *Journal of Solid Mechanics* **3**: 183-197.

[18] Yazdanpanah O., Seyedpoor S., 2015, A new damage detection indicator for beams based on mode shape data, *Structural Engineering and Mechanics* **53**(4): 725-744.

[19] Chen D., Yang J., Kitipornchai S., 2016, Free and forced vibrations of shear deformable functionally graded porous beams, *International Journal of Mechanical Sciences* **108**: 14-22.

[20] Pagani A., Carrera E., 2017, Large-deflection and post-buckling analyses of laminated composite beams by Carrera Unified Formulation, *Composite Structures* **170**: 40-52.

[21] Wang Y.Q., Zu J.W., 2017, Vibration behaviors of functionally graded rectangular plates with porosities and moving in thermal environment, *Aerospace Science and Technology* **69**: 550-562.

[22] Wang Y.Q., Zu J.W., 2017, Nonlinear steady-state responses of longitudinally traveling functionally graded material plates in contact with liquid, *Composite Structures* **164**:130-144.

[23] Nakhaei A.M., Dardel M., Ghasemi M.H., 2018, Modeling and frequency analysis of beam with breathing crack, *Archive of Applied Mechanics* **88**(10): 1743-1758.
[24] Wang Y.Q., 2018, Electro-mechanical vibration analysis of functionally graded piezoelectric porous plates in the translation state, *Acta Astronautica* **143**: 263-271.
[25] Navabian N., Taghipour R., Bozorgnasab M., Ghasemi J., 2018, Damage evaluation in plates using modal data and firefly optimisation algorithm, *International Journal of Structural Engineering* **9**(1): 50-69.
[26] Mottaghian F., Darvizeh A., Alijani A., 2018, Extended finite element method for statics and vibration analyses on cracked bars and beams, *Journal of Solid Mechanics* **10**(4): 902-928.
[27] Soncco K., Jorge X., Arciniega R., 2019, Postbuckling analysis of functionally graded beams, *IOP Conference Series: Materials Science and Engineering*.
[28] Mottaghian F., Darvizeh A., Alijani A. A., 2019, Novel finite element model for large deformation analysis of cracked beams using classical and continuum-based approaches, *Archive of Applied Mechanics* **89**: 195-230
[29] Wang Y.Q., Ye C., Zu J.W., 2019, Nonlinear vibration of metal foam cylindrical shells reinforced with graphene platelets, *Aerospace Science and Technology* **85**: 359-370.
[30] Li H-C., Ke L-L., Yang J., Kitipornchai S., Wang Y-S., 2020, Free vibration of variable thickness FGM beam submerged in fluid, *Composite Structures* **233**: 111582.
[31] Wang Y., Xie K., Fu T., 2020, Vibration analysis of functionally graded graphene oxide-reinforced composite beams using a new Ritz-solution shape function, *Journal of the Brazilian Society of Mechanical Sciences and Engineering* **42**(4): 1-14.
[32] Salmalian K., Alijani A., Azarboni H. R., 2021, A lagrange multiplier-based technique within the nonlinear finite element method in cracked columns, *Periodica Polytechnica Civil Engineering* **65**(1): 84-98.
[33] Mindlin R.D., 1951, Influence of rotatory inertia and shear on flexural motions of isotropic, elastic plates, *Journal of Applied Mechanics* **18**: 31-38.
[34] Navabian N., Bozorgnasab M., Taghipour R., Yazdanpanah O., 2016, Damage identification in plate-like structure using mode shape derivatives, *Archive of Applied Mechanics* **86**(5): 819-830.
[35] Wahab M.A., De Roeck G., 1999, Damage detection in bridges using modal curvatures: application to a real damage scenario, *Journal of Sound and Vibration* **226**(2): 217-235.